Laryngoscope
Investigative Otolaryngology

ORIGINAL RESEARCH OPEN ACCESS

Evaluation of the Effect of Platelet-Rich Plasma Injection After Recurrent Nerve Injury in Rats

Adem Senturk[1] | Ahmet Tarik Harmantepe[2] | Mevlut Yordanagil[3] | Bilgehan Celik[4] | Ozcan Budak[5] | Songul Doganay[6] | Fatih Turan[7] | Alp Omer Canturk[8] | Recayi Capoglu[8] | Fuldem Mutlu[9]

[1]Sakarya University Training and Research Hospital and Department of Surgical Oncology, Sakarya, Turkey | [2]Department of General Surgery, Sakarya University Faculty of Medicine, Sakarya, Turkey | [3]Department of Surgical Oncology, Kocaeli City Hospital, Kocaeli, Turkey | [4]Department of Otorhinolaryngology, Darıca Farabi Training and Research Hospital, Kocaeli, Turkey | [5]Department of Histology and Embryology, Sakarya University Faculty of Medicine, Sakarya, Turkey | [6]Department of Physiology, Sakarya University Faculty of Medicine, Sakarya, Turkey | [7]Department of Otorhinolayngology, Sakarya University Training and Research Hospital, Sakarya, Turkey | [8]Department of General Surgery, Sakarya University Training and Research Hospital, Sakarya, Turkey | [9]Department of Radiology, Sakarya University Faculty of Medicine, Sakarya, Turkey

Correspondence: Ahmet Tarik Harmantepe (tarikharmantepe@gmail.com)

Received: 15 November 2024 | **Revised:** 27 December 2024 | **Accepted:** 12 January 2025

Funding: The authors received no specific funding for this work.

Keywords: laryngeal nerve | nerve healing | nerve injury | platelet-rich plasma | thyroidectomy

ABSTRACT

Introduction: Injuries to the recurrent laryngeal nerve (RLN) that may occur during thyroidectomy cause hoarseness, dysphagia, and dyspnea. Even if the injured nerve can be repaired surgically, it heals slowly and not completely. Platelet-rich plasma (PRP) is obtained by centrifuging blood taken from the human body. PRP accelerates the healing of the injured nerve due to the many growth factors it contains. The aim of this study is to investigate the therapeutic effectiveness of PRP and assess surgical repair after RLN injury.

Materials and Methods: Twenty-eight male Wistar albino rats were used in this study. We divided the rats into four groups, with seven animals in each group. Group 1: RLN was cut and primary repair was performed. Group 2: RLN was cut but not repaired. Group 3: RLN was cut, primary repair was performed, and PRP was injected. Group 4: RLN was cut, and PRP was injected without repair. Laryngoscopy and electromyography (EMG) were conducted before and after the procedure. For histopathological evaluation, parameters such as Schwann cell count, axon damage, and immunohistochemical staining intensity of Ki-67 cell proliferation marker were examined.

Results: The highest amplitudes in EMG were seen in Group 3 rats at the third- and sixth-week postoperatively ($p < 0.05$). Regarding histopathological evaluation, Schwann cell count, and Ki-67 immunohistochemical staining were primarily observed in Group 3 rats ($p < 0.05$). Axonal damage and cytoplasmic vacuolization were minimally detected in Group 3 rats ($p < 0.05$).

Conclusion: In our experimental rodent model, PRP injection increased the Schwann cell count and cell proliferation rate in the injured RLN area by promoting the healing of nerve axons.

1 | Introduction

Peripheral nerves have better regeneration properties after damage compared to the central nervous system. The axons of peripheral nerves can regenerate, especially due to Schwann cells. However, in order for regeneration to occur, the injured nerve endings must come into contact with each other. One of the most common causes of peripheral nerve damage is

iatrogenic injuries. In such a scenario, which significantly impairs the quality of life of patients, the injured nerve can be repaired with various surgical procedures [1, 2].

Injury to the recurrent laryngeal nerve (RLN), which may occur during thyroid gland surgery, disrupts vocal cord movements and causes symptoms such as hoarseness, dysphagia, and dyspnea [3]. RLN repair can be conducted by various methods. If the RLN damage extends to <5 mm, direct anastomosis can be performed; alternatively, nerve guidance channels can be used, ansa cervicalis-to-RLN anastomosis, vagus to recurrent nerve anastomosis, or a free nerve graft can be applied. When a graft is used, two anastomoses are made. The nerves most commonly used as grafts are the greater auricular nerve, ansa cervicalis, transcervical nerves, and supraclavicular nerves [4–6]. Complications such as scar, neuroma, and donor site morbidity may develop after surgical procedures, especially due to nerve transplantation. Various methods are being developed to improve the outcome of surgical procedures. These include the use of growth factors for the regeneration of axons and the transplantation of replacement cells, such as Schwann cells, to the injured area [7–9].

Platelet-rich plasma (PRP) is obtained safely from whole blood. There are no known side effects or complications after clinical use of PRP [10]. Additionally, PRP is a very economical and effective treatment method [11]. When PRP is injected into the transected peripheral nerve area, tissue fibrinolysis occurs. Then, neurotrophic signaling molecules such as NGF, BDGF, and HGF and neurotrophic factors such as fibrin and fibronectin are secreted. In the next step, nerve repair begins with the triggering of chemotaxis, angiogenesis, and cell proliferation [12, 13]. As shown in an animal experimental study, regeneration of neurons occurs more frequently when PRP is applied along with surgical repair of the injured RLN [14].

The aim of this study was to investigate the therapeutic effectiveness of PRP after RLN injury.

2 | Materials and Methods

Ethical approval was received from the Sakarya University Animal Experiments Local Ethics Committee (06/05/2020–25). This study was conducted at Sakarya University Experimental Medicine Research and Application Unit, Turkey, between December 10, 2020 and January 21, 2021. Twenty-eight male Wistar albino rats weighing between 250 and 300 g and having normal laryngeal functions were used in the study. The rats were fed and monitored in open cages under standard laboratory conditions (temperature 23°C ± 2°C, humidity 45%–65%, 12-h day/night cycle) according to international guidelines for animal care and experimentation.

2.1 | Experimental Groups

The rats were divided into four groups with seven animals in each group. The RLNs of the rats in Group 1were cut, and primary repair was performed. Rats in Group 2 underwent RLN transection, but no primary repair was performed. Rats in Group 3 underwent primary repair after nerve transection, and PRP was injected. In Group 4, PRP was injected without primary nerve repair.

Group 1: RLN was cut and repaired (sutured) + no additional treatment.

Group 2: RLN was cut but left unsutured + no additional treatment.

Group 3: RLN was cut and repaired (sutured) + PRP treatment.

Group 4: RLN was cut and left unsutured + PRP treatment.

2.2 | Surgical Procedure

At the beginning of the procedure, each animal was anesthetized by subcutaneously injecting 45 mg/kg ketamine (Ketalar; Pfizer, Istanbul, Turkey) and 5 mg/kg xylazine (Rompun; Bayer, Istanbul, Turkey) after 4–6 h of food restriction. All animals underwent laryngoscopic examination before the procedure and it was observed that both vocal cord movements were normal. Additionally, transoral laryngeal electromyography (EMG) recordings were made to be used as the baseline value. Rats breathed room air throughout the entire surgical procedure. The surgical area was shaved and prepared aseptically for surgery. A vertical incision of approximately 2 cm was made from the mentum to the sternum in the midline of the neck with a size 15 scalpel. After the skin and subcutaneous area was traversed, the salivary glands were gently retracted laterally for a clear visualization of the surgical field, and to reach the trachea in the midline through the stretch muscles (Figure 1a). At this stage, the left RLN was identified in the tracheoesophageal groove and dissected (Figure 1b). The left RLN of all rats in the group was transected. Additionally, after the incision, the nerves of the rats in Groups 1 and 3 were sutured to the primary epineural nerve with 10.0 prolene suture (Figure 1c). Finally, PRP was injected in rats of Groups 3 and 4, as stated in the PRP application sub-section below. After the suspensory muscles and skin were sutured, the surgical area was closed, and the operation was completed (Figure 1d).

2.3 | Laryngoscopy Procedure

For laryngoscopy, all rats were placed in a supine position under anesthesia and then in the reverse Trendelenburg position with a 15° inclination. A 3.0 silk suture was passed through the anterior middle one-third of the tongue, and the tongue was pulled and suspended to provide a better field of view. Vocal fold movements were evaluated with a 0°3.0-mm auto endoscope (R11573A); Karl Storz (Karl Storz Endoskope, Tuttlingen, Germany). Vocal fold movements were scored for standardization where 0 denoted completely motionless, 1 denoted reduced movement in the vocal fold, and 2 denoted normal vocal fold movement (Table 1). During the amplitude flow, the vocal cords were simultaneously evaluated observationally with a laryngoscope. Both EMG and observational methods were used for the subsequent analysis of data.

2.4 | EMG Procedure

All rats underwent transoral laryngeal EMG during a spontaneous, unstimulated respiratory cycle during sleep under general anesthesia. After vocal cord examination under anesthesia,

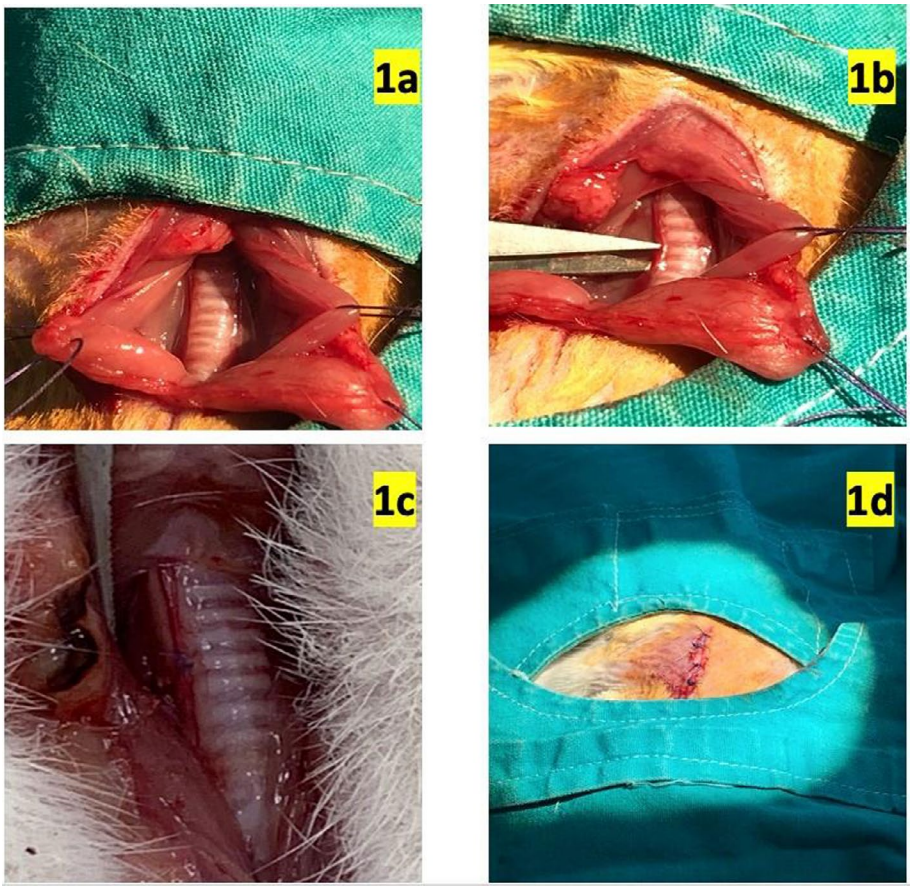

FIGURE 1 | Surgical procedure.

TABLE 1 | Scoring for vocal fold movements.

Vocal fold movements	Score
Completely motionless	0
Reduced movement	1
Normal movement	2

the EMG electrode was placed on the left posterior cricoarytenoid muscle. A ground electrode was placed on the right pectoralis major muscle of rats. The screen sweep speed was set to 10 ms/division, and screen sensitivity was set to 100 mV. EMG recordings were taken for all rats before the surgical procedure, immediately after the surgical procedure, at the third- and the sixth-week postoperatively (Figure 2a–c).

2.5 | PRP Preparation

After the donor rat was anesthetized by subcutaneously injecting 45 mg/kg ketamine (Ketalar; Pfizer, Istanbul, Turkey) and 5 mg/kg xylazine (Rompun; Bayer, Istanbul, Turkey), approximately 5 mL of fresh blood was obtained by puncturing the heart of the donor rat, for a planned homologous transfer, and was placed in a tube containing sodium citrate. The blood was first centrifuged at 400× *g* for 10 min at 21°C–22°C. Next, the blood was separated into three layers: acellular plasma at the top, platelets in the middle, and white blood cells and erythrocytes at the bottom. The top two layers were pipetted into another tube and centrifuged again at 800× *g* for 10 min. After the second centrifugation, two layers were formed: acellular plasma on top and PRP at the bottom. Approximately three-quarters of the acellular plasma was aspirated with a pipette, and the remaining portion (approximately 0.8 mL of PRP) was removed from the bottom of the tube. The number of platelets, erythrocytes, and leukocytes present in the prepared PRP sample and in rat whole blood were counted with an automatic cell counter. No complications were encountered during the procedure. The donor animal used for homologous transfer was sacrificed after completion of surgery.

2.6 | PRP Application

After the left RLN was transected and sutured in Group 3 rats, and after the left RLN was transected in Group 4 rats, 0.05-mL PRP was injected using a 1 mL syringe and a 27-gauge needle. The wound was then closed as described above.

Based on previous studies, we decided that a 6-week follow-up period was sufficient for vocal cord evaluation [15–18]. After a 6-week recovery period, all rats were sacrificed using the cervical dislocation method and the larynx and tracheal tissues were removed. Histopathological examinations were conducted under a light microscope at 40×, 100×, and 200× magnifications. Eight serial sections were carefully selected from each experimental group, six consecutive areas of each cross-section were counted, and mean values were determined numerically.

2.7 | Histopathological Procedure

The rat tissues were placed in a 10% buffered neutral formaldehyde solution and fixed for 48 h. After the fixation period, the tissues were removed from the formalin solution and kept in nitric acid solution to decalcify. When the tissues became soft enough to be sectioned, they were dehydrated with alcohol, clarified with xylol, embedded in paraffin, and subjected to routine tissue processing. Tissue samples, whose tissue processing was complete, were embedded in paraffin. Tissue sections of 4-μm thickness were prepared from the paraffin blocks and placed onto polylysine-coated glass slides by employing a Thermo Scientific HM 355S brand microtome (Thermo Fisher Scientific, Waltham, MA, USA). For hematoxylin–eosin

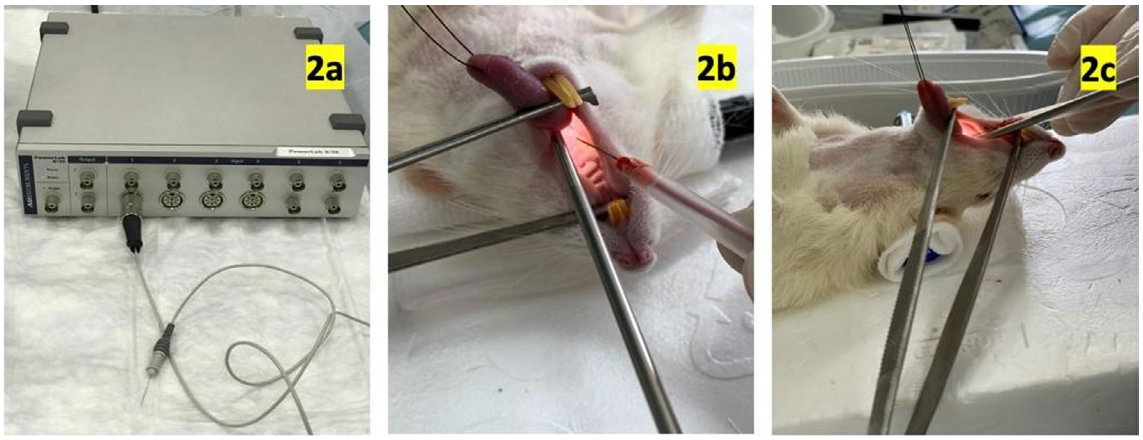

FIGURE 2 | Transoral laryngeal EMG recording.

TABLE 2 | Weight changes of all groups over time.

		Group 1	Group 2	Group 3	Group 4	
		Mean ± SD	Mean ± SD	Mean ± SD	Mean ± SD	*p*
Weight	Preop	318.14 ± 17.43	370.29 ± 47.91	—	—	0.012*
	1 Week	311.43 ± 18.62	372.29 ± 51.31	433.43 ± 31.25	327.29 ± 27.61	—
	2 Week	322.43 ± 17.08	377.71 ± 50.81	437.14 ± 36.42	337.57 ± 25.90	< 0.05* $p^{1-2} = 0.041$ $p^{1-3} < 0.001$ $p^{2-3} = 0.013$ $p^{3-4} = 0.024$
	3 Week	334.57 ± 16.01	385.71 ± 50.99	444.00 ± 34.90	346.29 ± 25.66	< 0.05* $p^{1-2} = 0.047$ $p^{1-3} < 0.001$ $p^{2-3} = 0.018$ $p^{3-4} = 0.036$
	4 Week	343.43 ± 18.20	389.14 ± 50.28	458.86 ± 34.52	359.14 ± 29.10	< 0.05* $p^{1-3} < 0.001$ $p^{2-3} = 0.021$ $p^{3-4} = 0.044$
	5 Week	353.00 ± 18.65	394.71 ± 48.08	469.43 ± 32.74	369.29 ± 33.91	< 0.05* $p^{1-3} < 0.001$ $p^{2-3} = 0.027$ $p^{3-4} = 0.031$
	6 Week	360.29 ± 18.64	398.86 ± 51.11	472.00 ± 32.28	371.86 ± 30.68	< 0.05* $p^{1-3} < 0.001$ $p^{2-3} = 0.032$ $p^{3-4} = 0.047$

*One way Anova test, $p < 0.05$ statistical significance.

TABLE 3 | Vocal fold movement changes over time in all groups.

			Group 1	Group 2	Group 3	Group 4	
			n (%)	*n* (%)	*n* (%)	*n* (%)	*p*
Vocal cord (VC)	VC Preop	Completely motionless	0	0	0	0	—
		Decreased movement in VC	0	0	0	0	
		Normal VC movement	7	7	7	7	
	VC Postop	Completely motionless	7	7	7	7	—
		Decreased movement in VC	0	0	0	0	
		Normal VC movement	0	0	0	0	
	VC 3 week	Completely motionless	6	6	5	5	0.741
		Decreased movement in VC	1	1	2	2	
		Normal VC movement	0	0	0	0	
	VC 6 week	Completely motionless	4	6	4	4	0.326
		Decreased movement in VC	2	1	2	3	
		Normal VC movement	1	0	1	0	

Note: Chi-square test, *n*: sayı, %: Yüzde, $p < 0.05$ statistical significance.

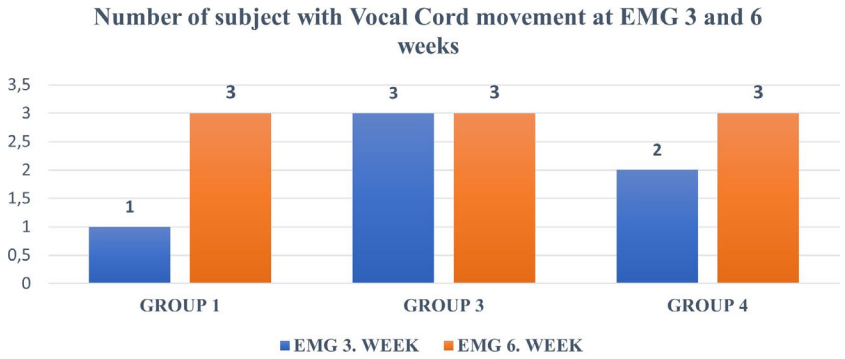

CHART 1 | Number of subjects with vocal cord movement at EMG 3 and 6 weeks.

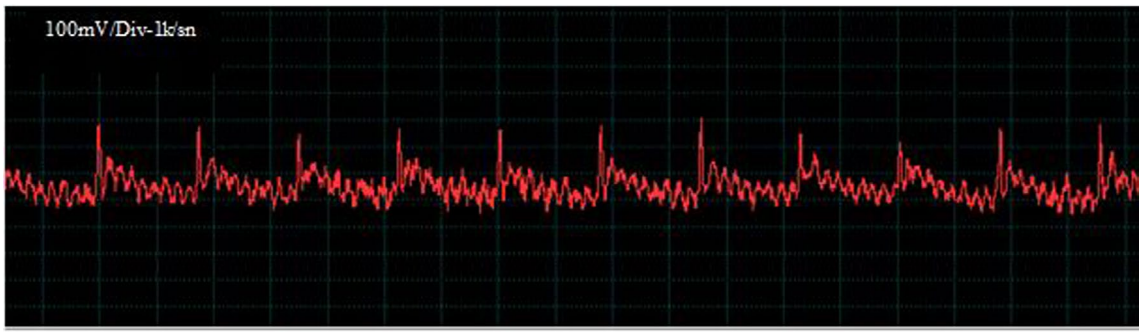

FIGURE 3 | EMG during spontaneous breathing in an anesthetized rat. It is seen that the MUP amplitudes of the action potentials of the motor units are normal.

(Bio-Optica, Milan, Italy) staining, the sections were placed on grinding slides and kept at room temperature to dry until the staining process. Some of the tissue samples were examined by immunofluorescence for myelin protein zero and Ki-67 staining intensity.

2.8 | Statistical Evaluation

SPSS (statistical package for social sciences) software version 26 was used for statistical analysis. Mean ± standard deviation values were used for continuous variables, and percentage values were

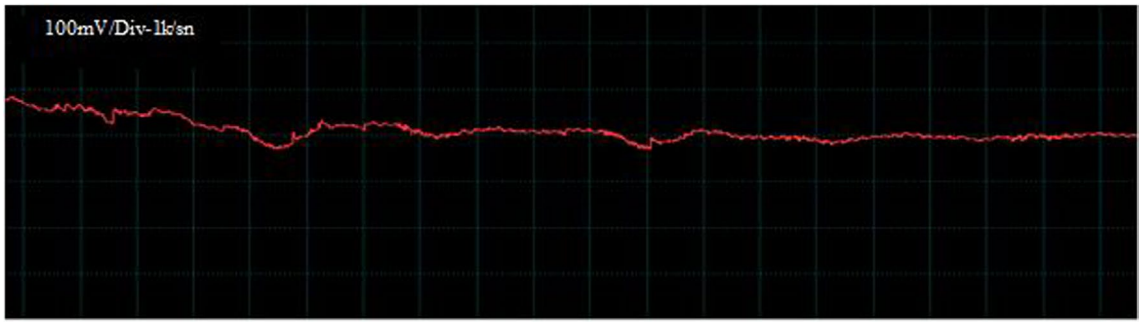

FIGURE 4 | EMG recording taken immediately after nerve incision. It can be seen that there are no MUP amplitudes.

TABLE 4 | EMG test results of all groups over time.

	Group 1	Group 2	Group 3	Group 4	
	Mean ± SD	Mean ± SD	Mean ± SD	Mean ± SD	
	Median [Q_L–Q_U]	Median [Q_L–Q_U]	Median [Q_L–Q_U]	Median [Q_L–Q_U]	*p*
EMG Preop	2.47 ± 0.38 2.44 [1.78–2.99]	2.54 ± 0.24 2.59 [2.23–2.89]	2.53 ± 0.27 2.54 [2.29–2.99]	2.48 ± 0.33 2.48 [1.99–2.96]	0.841
EMG Postop	—	—	—	—	—
EMG 3 week	0.07 ± 0.17 0 [0–0.46]	—	0.21 ± 0.28 0 [0–0.58]	0.14 ± 0.24 0 [0–0.58]	< 0.05* p^{1-3} < 0.001 p^{1-4} < 0.001 p^{3-4} = 0.012
EMG 6 week	0.30 ± 0.54 0 [0–0.58]	—	0.33 ± 0.47 0 [0–1.18]	0.23 ± 0.29 0 [0–0.60]	< 0.05* p^{1-3} = 0.042 p^{3-4} = 0.039
p	< 0.001*		< 0.001*	< 0.001*	

*One way Anova test, $p < 0.05$ statistical significance.

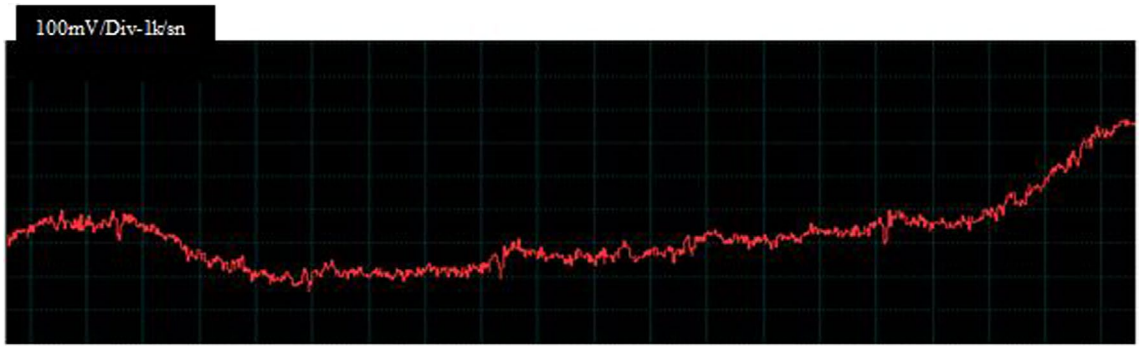

FIGURE 5 | EMG recordings taken at the third postoperative week. It is seen that irregular and low amplitude MUPs are formed.

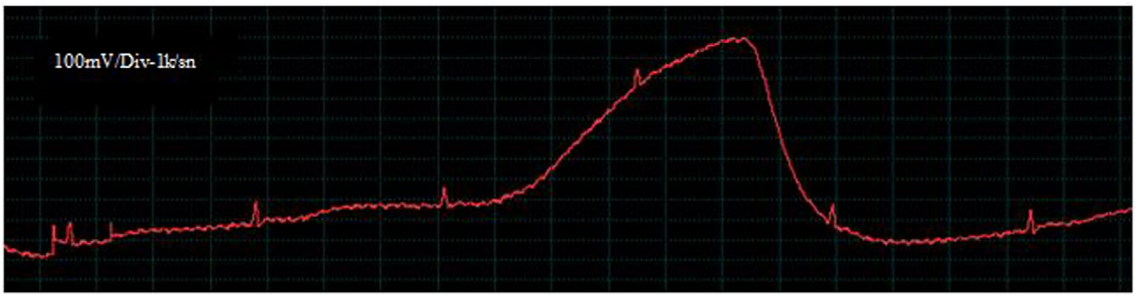

FIGURE 6 | EMG recordings taken at the third postoperative week. It is observed that irregular and low amplitude MUP occurs.

used for categorical variables. First, for the comparison of numerical data, compliance with normal distribution was checked with the Kolmogorov Smirnov test. Based on this analysis, it was decided to use non-parametric tests. Kruskal Wallis tests were used for numerical comparisons between groups, and chi-square tests were used for categorical comparisons. Post hoc analysis was performed if statistical significance was achieved in multiple comparisons. $p < 0.05$ was considered sufficient for statistical significance.

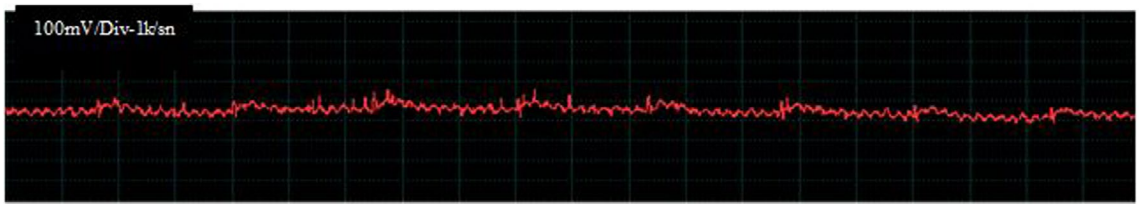

FIGURE 7 | EMG recordings taken at the sixth postoperative week. It is observed that MUP amplitudes occur more frequently and regularly compared to the third week.

TABLE 5 | Histological and immunohistochemical results of all groups.

	Group 1	Group 2	Group 3	Group 4	
	Mean ± SD	Mean ± SD	Mean ± SD	Mean ± SD	
	Median [Q_L–Q_U]	Median [Q_L–Q_U]	Median [Q_L–Q_U]	Median [Q_L–Q_U]	*p*
Schwann cell count	14.43 ± 1.27 15.00 [12.0-16.0]	9.00 ± 0.82 9.00 [8.0-10.0]	17.43 ± 1.39 17.0 [16.0-20.0]	11.71 ± 1.81 12.0 [10.0-13.0]	< 0.001* $p^{1-2} = 0.023$ $p^{1-3} = 0.035$ $p^{2-3} = 0.005$ $p^{2-4} = 0.048$ $p^{3-4} = 0.011$
Axon damage	8.00 ± 0.82 8.0 [7.0-9.0]	15.29 ± 1.12 15.0 [14.0-17.0]	5.86 ± 1.35 5.00 [4.0-8.0]	9.00 ± 1.29 9.0 [7.0-11.0]	< 0.001* $p^{1-2} = 0.002$ $p^{1-3} = 0.049$ $p^{2-3} = 0.003$ $p^{2-4} < 0.001$
Cytoplasmic vacuolization	5.43 ± 0.98 5.0 [4.0-7.0]	11.71 ± 1.50 12.0 [10.0-14.0]	5.00 ± 0.82 5.00 [4.0-6.0]	8.00 ± 0.82 8.0 [7.0-9.0]	< 0.001* $p^{1-2} = 0.007$ $p^{1-4} = 0.041$ $p^{2-3} = 0.019$ $p^{2-4} = 0.036$
Ki-67 connective tissue	20.43 ± 1.72 20.0 [18.0-23.0]	11.29 ± 1.25 12.0 [10.0-13.0]	28.43 ± 1.27 28.00 [3.0-27.0]	19.71 ± 1.80 20 [17.0-22.0]	< 0.001* $p^{1-2} = 0.001$ $p^{1-3} = 0.029$ $p^{2-4} < 0.001$ $p^{3-4} = 0.002$
P0 protein-RLS	18.29 ± 1.89 18.0 [16.0-22.0]	13.86 ± 1.36 14.0 [12.0-16.0]	33.43 ± 1.39 33.00 [32.0-36.0]	23.72 ± 0.95 24 [22.0-25.0]	< 0.001* $p^{1-2} = 0.016$ $p^{1-3} < 0.001$ $p^{2-3} < 0.001$ $p^{2-4} < 0.001$ $p^{3-4} < 0.001$
Ki-67 vocal cord	11.71 ± 1.11 11.0 [10.0-13.0]	7.43 ± 0.98 7.0 [6.0-9.0]	12.57 ± 1.81 12.00 [10.0-15.0]	12.71 ± 1.11 13 [11.0-14.0]	< 0.001** $p^{1-2} = 0.003$ $p^{2-3} = 0.014$ $p^{2-4} < 0.001$

Abbreviations: Q_L: lower quartile, Q_U: upper quartile, SD: standard deviation.
*One way Anova test, $p < 0.05$ statistical significance.
**Kruskal Wallis H test, $p < 0.05$ statistical significance.

3 | Results

When the weight changes of all groups were examined over time (Table 2), it was observed that the highest weight gain at all times was in Group 3 animals and the least weight gain was in Group 2 rats. The mean weight differences between the groups were statistically significant at all times ($p < 0.001$) (Table 2).

3.1 | Laryngoscopic Findings

Although all experimental groups had normal vocal fold movement in the preoperative period, the vocal cords of rats in all groups were completely immobile in the postoperative period.

During a 3-week postoperative evaluation period, vocal fold movements were completely absent in most rats, while some vocal fold movements were observed in a small number of rats. At the sixth-week assessment of experimental groups, a reduction in vocal fold movement was observed in most of the rats in all four groups, while normal vocal fold movement was observed in one rat each in Groups 1 and 4. However, the differences in vocal fold movement were not statistically significant ($p = 0.741$, $p = 0.326$) (Table 3; Chart 1).

3.2 | EMG Findings

It was observed that the motor unit potential (MUP) amplitude values of all rats in all four experimental groups were normal in the transoral laryngeal EMG tests performed before the procedure (Figure 3). In addition, it was observed that the preoperative mean amplitude values of rats in Groups 2 and 3 were higher than those of rats in Groups 1 and 4; however, these differences between the groups were not statistically significant ($p = 0.841$). It was observed that the MUP amplitudes of all groups disappeared in the postoperative period, as expected (Figure 4).

In addition, when the temporal change of amplitude values in Groups 1, 3, and 4 were examined, a statistically significant difference was detected between the MUP amplitude values calculated in the third and sixth weeks compared with the preoperative period ($p < 0.05$) (Table 4).

In the EMG recordings made in the third week, an MUP amplitude was observed in one animal in Group 1 (in whom vocal cord movement was observed figure endoscopically), in three animals in Group 3, and in two animals in Group 4. In the other rats of Group 1, 3, and 4, no vocal cord movement was observed and an MUP amplitude could not be detected via EMG.

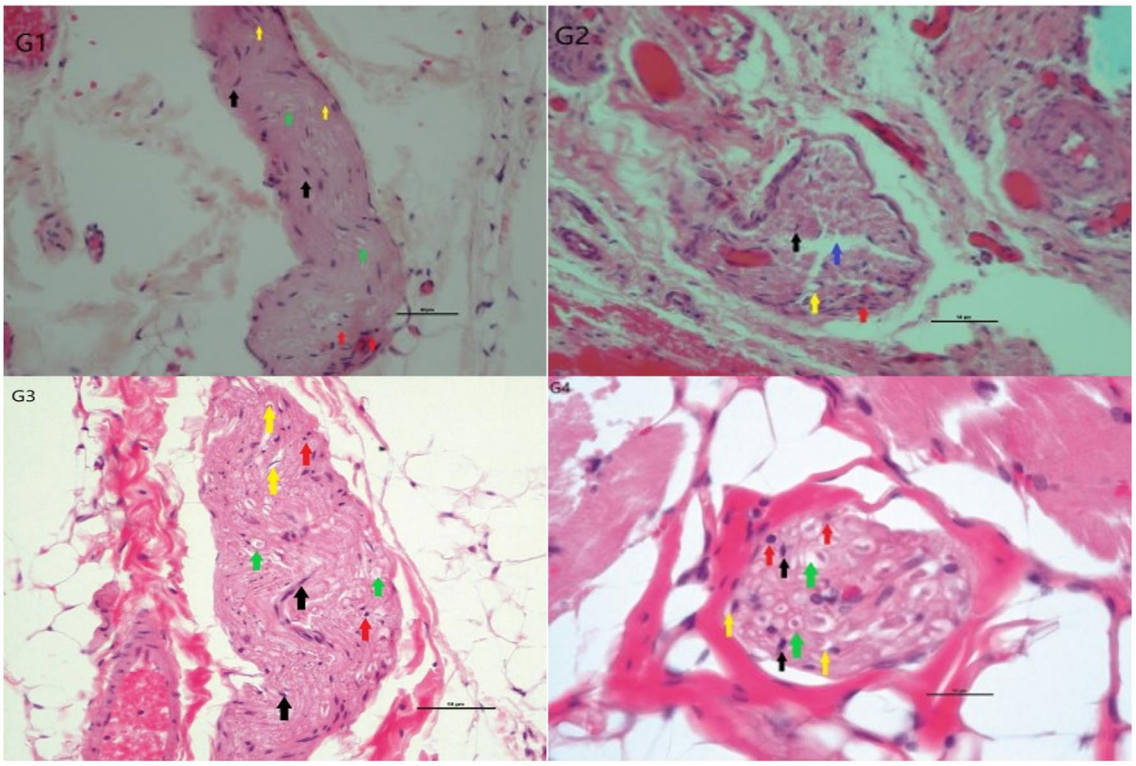

FIGURE 8 | Groups H.E. peripheral nerve images, 50 scale bar 200× images. In the G1 group, pyknotic neuron cells are seen and Schwann cells are seen occasionally. The epineurium layer around the nerve tissue has begun to be organized. In the G2 group, the untreated and unsutured group, disintegration of the nerve tissue is observed. Schwann cells were less numerous than the G1 group, and damaged pyknotic neuron cells were seen. In the G3 group, which was sutured and given PRP, Schwann cell numbers were higher than the other groups. The epineurium layer was observed to be enlarged. Schwann cells were seen after G4 PRP treatment. Very few pyknotic neuron cells were seen. The epineurium layer is in its normal arrangement around the nerve tissue. Black arrow (Schwann cells), red arrow (damaged neuron cells with pyknotic nuclei), yellow arrow (cytoplasmic vacuolization), green arrows (axon damage), and blue arrow (fragmented nerve tissue damage).

In the EMG recordings made in the sixth week, we observed that MUP amplitudes and voltage values increased in three animals of Group 1, in three animals of Group 3, and in three rats in Group 4 in whom vocal cord movement was observed endoscopically. For the other rats in Groups 1, 3, and 4, no vocal cord movement was observed and MUP amplitude could not be detected via EMG. An MUP amplitude was not obtained in any of the animals in Group 2 at the third and sixth weeks.

In the statistical comparison of the MUP amplitude values of animals in Groups 1, 3, and 4, where an MUP amplitude had been detected in the third and sixth weeks, it was observed that MUP amplitude values were higher for rats in Groups 3 and 4 and these higher amplitude values were statistically significant ($p < 0.05$).

In the postoperative EMG recordings taken at the third week after nerve repair, irregular and low-amplitude MUPs were observed in some of the rats in Groups 1 and 4 (Figures 5 and 6).

In the postoperative EMG recordings taken at the sixth week after nerve repair, it was seen that MUPs occurred more frequently compared with the third week postoperative data and their amplitudes were at higher voltage values compared to the third week postoperative data (Figure 7). Additionally, it was observed that MUPs began occurring in a higher number of rats in Group 1 in the sixth postoperative week.

3.3 | Histopathological Findings

Histopathological examinations were conducted under a light microscope at 40×, 100×, and 200× magnifications. Eight serial sections were carefully selected from each experimental group, and the mean values were numerically determined by counting six consecutive areas of each cross-section. When the area around the RLN was examined with hematoxylin–eosin staining, many Schwann cells were seen in animals of Groups 1 and 3, while fewer Schwann cells were observed in Groups 2 and 4 compared with Groups 1 and 3. When Schwann cell number was evaluated statistically between groups, a significant difference was seen ($p < 0.001$).

When the area surrounding the RLN was examined by hematoxylin–eosin staining, neuron with pyknotic nucleus and occasional Schwann cells were observed in Group 1 rats, and it was observed that the epineurium layer had begun to heal. In Group 2 rats, nerve tissue fragmentation was observed, Schwann cells were less common than in Group 1, and damaged neuron with pyknotic nucleus were observed. In Group 3, Schwann cell counts were low, and the epineurium layer was enlarged. In Group 4, a large number of Schwann cells and very few neuron with pyknotic nucleus were visible. The epineurium layer was in its normal arrangement around the nerve tissue.

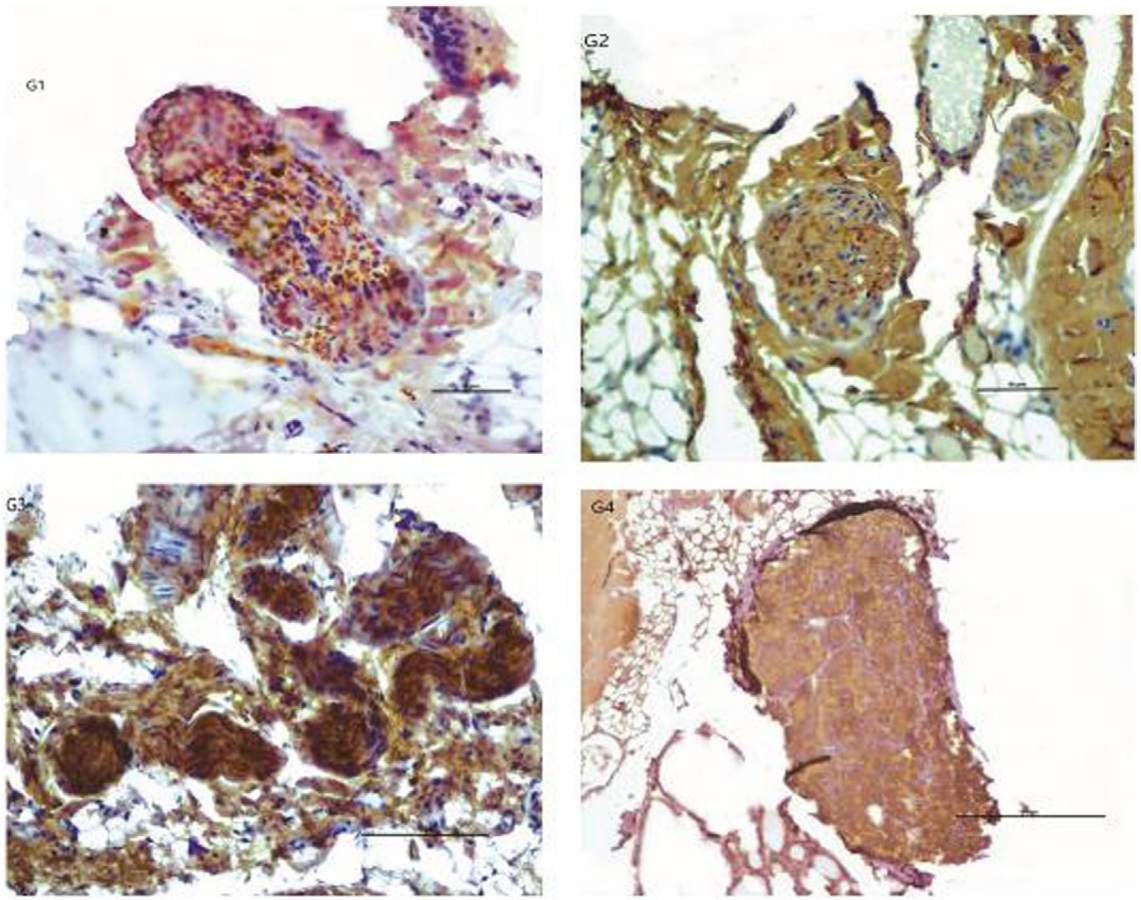

FIGURE 9 | PO immunohistochemistry staining preparations of groups in the area of peripheral nerve damage, 50 scale bars. 200× magnification. Group 3 had the highest PO staining intensity, then Group 1 and Group 4, and the lowest PO staining intensity was observed in Group 2. The lower Po density in the unsutured and untreated G2 group is due to the low number of Schwann cells in the tissue.

When the groups were compared in terms of axon damage and cytoplasmic vacuolization in the nerve injury area, it was observed that the most damage was visible in Group 2 animals and the least damage was present in Group 3. When compared in terms of myelin protein zero and Ki-67 staining intensity, it was seen that these were highest in Group 3 and lowest in Group 2. The differences between groups were statistically significant for all histopathological examinations ($p < 0.001$) (Table 5).

When groups were compared in terms of axon damage, cytoplasmic vacuolization, myelin protein zero, and Ki67 staining intensity in the nerve transected area, we observed that these parameters values were highest in Group 2 and lowest in Group 4. As a result of the histopathological examination of the vocal cords, Group 4 animals showed the highest Ki-67 staining intensity, whereas the lowest KI-67 staining intensity was found in Group 2 animals. In addition, Group 4 animals displayed the thickest epithelial, connective tissue, and muscle layers among all groups, whereas the thinnest such layers were found in Group 2 rats. The vocal cords were found to be thicker in the groups that underwent primary suture repair. When Ki-67 staining intensity was evaluated in the vocal cords, there was a statistically significant difference between the groups.

Histopathological examination results are shown with explanations in Figures 8–11.

4 | Discussion

RLN injury is a significant complication of neck surgeries, leading to vocal cord atrophy, hoarseness, and aspiration. Our findings demonstrate that surgical nerve repair combined with PRP application promotes reinnervation and improves functional outcomes compared to no intervention.

We observed that vocal fold movement and MUP amplitudes improved significantly in rats undergoing primary nerve repair, with or without PRP. These findings align with prior studies highlighting the benefits of primary RLN repair in restoring laryngeal function through reinnervation [19, 20]. Importantly, the addition of PRP enhanced these outcomes, as evidenced by higher Schwann cell counts, reduced axonal damage, and greater Ki-67 staining in PRP-treated groups. These results support existing literature emphasizing PRP's regenerative properties due to its growth factor content, including PDGF, VEGF, and IGF-1, which promote Schwann cell proliferation and axonal regeneration [21–24].

PRP's role in enhancing neovascularization is another critical mechanism contributing to peripheral nerve repair. Growth factors such as VEGF stimulate angiogenesis, improving the migration of Schwann cells and facilitating axonal recovery [13, 24]. In our study, Group 3 (nerve repair + PRP) showed the highest Schwann cell counts and Ki-67 staining, highlighting

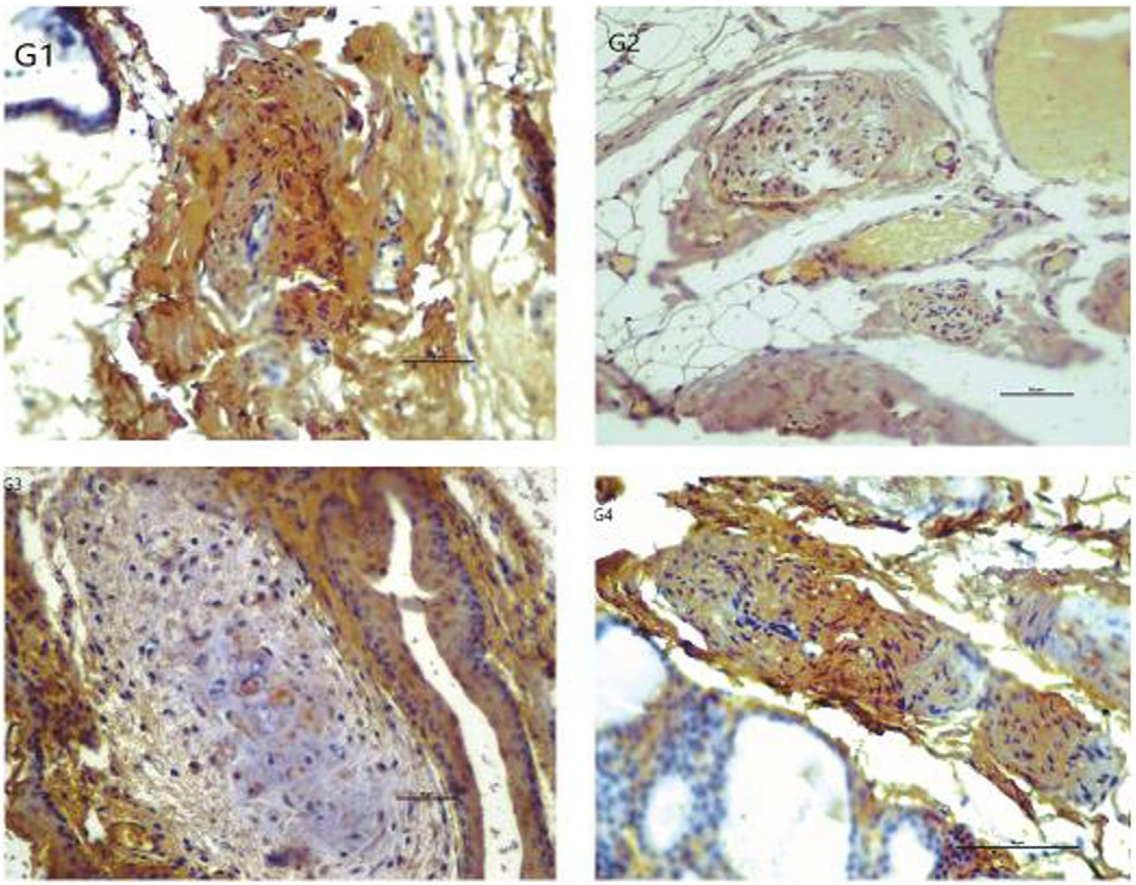

FIGURE 10 | Ki-67 immunohistochemistry staining preparations in the connective tissue area of the groups in the area of peripheral nerve damage, 50 scale bars. 200× magnification. Group 3 had the highest Ki-67 staining density, then Group 1 and Group 4, and the lowest Ki-67 staining density was seen in Group 2.

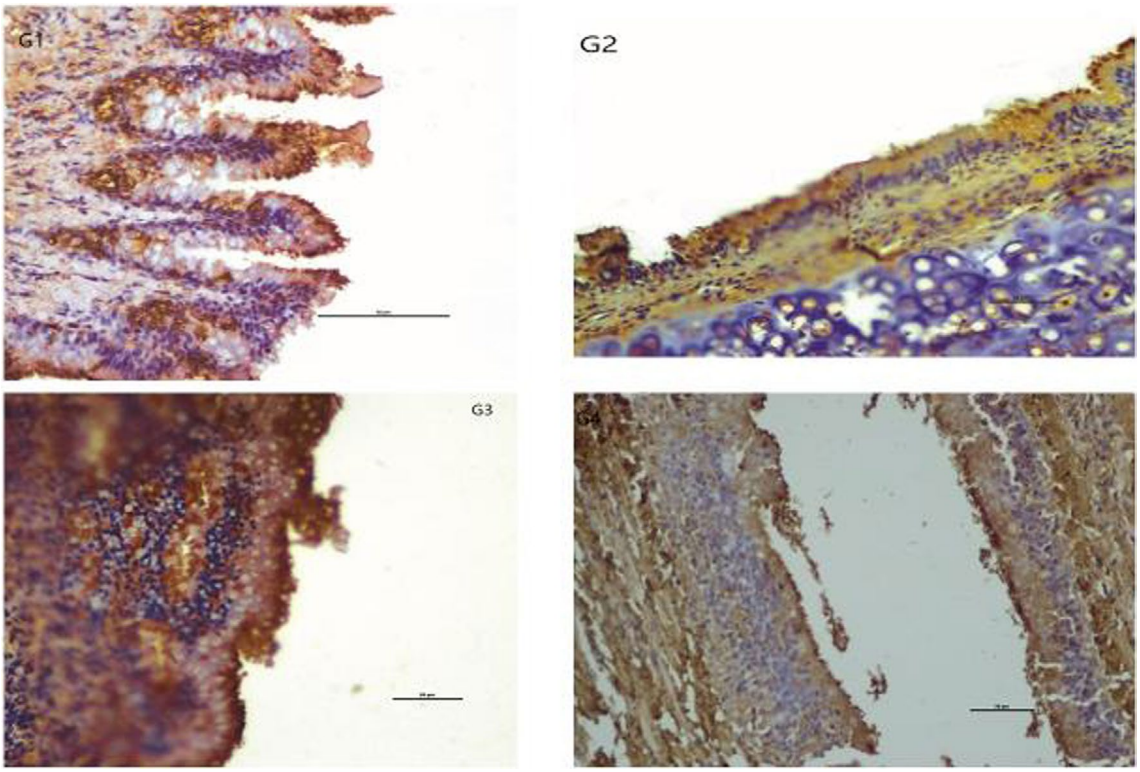

FIGURE 11 | Ki-67 immunohistochemistry staining preparations in the connective tissue area of the groups in the vocal cord area, 50 scale bars. 200× magnification. Group 3 had the highest Ki-67 staining density, then Group 1 and Group 3, and the lowest Ki-67 staining density was seen in Group 2. Additionally, in Group 3, the epithelial layer and the underlying connective tissue and muscle layer were the thickest. The thinnest layer was in Group 2, which was untreated and unsutured, then in Group 1 and Group 4. It was observed that the vocal cord was thicker in the groups, especially in the sutured tissues.

PRP's role in accelerating peripheral nerve healing. Similar studies have reported improved outcomes with PRP following nerve injury, especially when applied at optimal concentrations [13, 22]. The PRP concentration in our study (~900,000 platelets/μL) falls within the effective range suggested in prior research [24].

Although PRP's regenerative potential is well-established, factors such as the timing of PRP application and its dosage remain areas for further investigation. Zhu et al. demonstrated improved sciatic nerve recovery with multiple PRP doses [13]. In contrast, we applied PRP immediately post-injury as a single dose, which yielded promising results. Future studies are warranted to explore the effects of delayed or repeated PRP administration on RLN healing.

Histopathological analyses further reinforced our findings, revealing reduced axonal damage and enhanced Schwann cell proliferation in PRP-treated groups. These observations suggest that PRP not only accelerates nerve regeneration but also promotes structural recovery of the nerve and surrounding tissues. However, as TGF-β1 in PRP may inhibit axonal growth under certain conditions, further studies are needed to optimize PRP formulations for nerve repair [25].

Our study has some limitations. The exclusive use of male rats limits generalizability to females due to known sex-based differences in immune responses [26–28]. Our follow-up period was shorter (6 weeks) compared to some studies (12 weeks), which may have influenced long-term outcome assessments. Finally, while our PRP concentration was effective, its impact relative to other concentrations remains to be explored. Additionally, the inability to measure nerve conduction velocity and the lack of electrophysiological evaluations prevented a more comprehensive explanation of the effects of PRP on nerve regeneration.

5 | Conclusion

Our study demonstrates that surgical repair of RLN injury significantly improves functional and structural outcomes, and PRP application further enhances nerve regeneration by increasing Schwann cell proliferation and reducing axonal damage. These findings highlight PRP's potential as an adjunctive treatment in peripheral nerve injuries, warranting further investigation into its optimal concentration, timing, and long-term effects.

Acknowledgments

The authors have nothing to report.

Ethics Statement

This study was approved by the Faculty of Medicine, Sakarya University Ethics Committee.

Conflicts of Interest

The authors declare no conflicts of interest.

References

1. W. D. Rinkel, B. M. Huisstede, D. J. van der Avoort, J. H. Coert, and S. E. Hovius, "What Is Evidence Based in the Reconstruction of Digital Nerves? A Systematic Review," *Journal of Plastic, Reconstructive & Aesthetic Surgery* 66, no. 2 (February 2013): 151–164, https://doi.org/10.1016/j.bjps.2012.08.035.

2. E. A. Huebner and S. M. Strittmatter, "Axon Regeneration in the Peripheral and Central Nervous Systems," *Results and Problems in Cell Differentiation* 48 (2009): 339–351, https://doi.org/10.1007/400_2009_19.

3. L. H. Rosenthal, M. S. Benninger, and R. H. Deeb, "Vocal Fold Immobility: A Longitudinal Analysis of Etiology Over 20 Years," *Laryngoscope* 117, no. 10 (October 2007): 1864–1870, https://doi.org/10.1097/MLG.0b013e3180de4d49.

4. E. Papadopoulou, K. Sapalidis, S. Triaridis, and A. Printza, "The Role of Primary Repair of the Recurrent Laryngeal Nerve during Thyroid/Parathyroid Surgery in Vocal Outcomes—A Systematic Review," *Journal of Clinical Medicine* 12, no. 3 (February 2023): 1212, https://doi.org/10.3390/jcm12031212.

5. M. Fadhil, T. Havas, and I. Jacobson, "Timing of Ansa Cervicalis-to-recurrent Laryngeal Nerve Reinnervation: A Systematic Review," *Journal of Voice* 38 (June 2022): 1484–1497, https://doi.org/10.1016/j.jvoice.2022.04.010.

6. Q. Yuan, J. Hou, Y. Liao, L. Zheng, K. Wang, and G. Wu, "Selective Vagus-Recurrent Laryngeal Nerve Anastomosis in Thyroidectomy With Cancer Invasion or Iatrogenic Transection," *Langenbeck's Archives of Surgery* 405, no. 4 (June 2020): 461–468, https://doi.org/10.1007/s00423-020-01906-y.

7. M. B. De la Rosa, E. M. Kozik, and D. S. Sakaguchi, "Adult Stem Cell-Based Strategies for Peripheral Nerve Regeneration," *Advances in Experimental Medicine and Biology* 1119 (2018): 41–71, https://doi.org/10.1007/5584_2018_254.

8. Z. Kızılay, N. Kahraman Çetin, M. Aksel, et al., "Ozone Partially Decreases Axonal and Myelin Damage in an Experimental Sciatic Nerve Injury Model," *Journal of Investigative Surgery* 32, no. 1 (January 2019): 8–17, https://doi.org/10.1080/08941939.2017.1369606.

9. A. Fuentes-Flores, C. Geronimo-Olvera, K. Girardi, et al., "Senescent Schwann Cells Induced by Aging and Chronic Denervation Impair Axonal Regeneration Following Peripheral Nerve Injury," *EMBO Molecular Medicine* 15, no. 12 (December 2023): e17907, https://doi.org/10.15252/emmm.202317907.

10. S. Kotsovilis, N. Markou, E. Pepelassi, and D. Nikolidakis, "The Adjunctive Use of Platelet-Rich Plasma in the Therapy of Periodontal Intraosseous Defects: A Systematic Review," *Journal of Periodontal Research* 45, no. 3 (June 2010): 428–443, https://doi.org/10.1111/j.1600-0765.2009.01236.x.

11. J. L. Rutkowski, J. M. Thomas, C. L. Bering, et al., "Analysis of a Rapid, Simple, and Inexpensive Technique Used to Obtain Platelet-Rich Plasma for Use in Clinical Practice," *Journal of Oral Implantology* 34, no. 1 (2008): 25–33, https://doi.org/10.1563/1548-1336(2008)34[25:AAOARS]2.0.CO;2.

12. E. Anitua, R. Prado, M. Azkargorta, et al., "High-Throughput Proteomic Characterization of Plasma Rich in Growth Factors (PRGF-Endoret)-Derived Fibrin Clot Interactome," *Journal of Tissue Engineering and Regenerative Medicine* 9, no. 11 (November 2015): E1–E12, https://doi.org/10.1002/term.1721.

13. Y. Zhu, Z. Jin, J. Wang, et al., "Ultrasound-Guided Platelet-Rich Plasma Injection and Multimodality Ultrasound Examination of Peripheral Nerve Crush Injury," *npj Regenerative Medicine* 5, no. 1 (November 2020): 21, https://doi.org/10.1038/s41536-020-00101-3.

14. J. W. Kim, J. M. Kim, M. E. Choi, et al., "Platelet-Rich Plasma Loaded Nerve Guidance Conduit as Implantable Biocompatible Materials for Recurrent Laryngeal Nerve Regeneration," *npj Regenerative Medicine* 7, no. 1 (September 2022): 49, https://doi.org/10.1038/s41536-022-00239-2.

15. D. T. Edizer, Z. Dönmez, M. Gül, et al., "Effects of Melatonin and Dexamethasone on Facial Nerve Neurorrhaphy," *Journal of International Advanced Otology* 15, no. 1 (2019): 43.

16. A. Shiotani, H. Nakagawa, and P. W. Flint, "Modulation of Myosin Heavy Chains in Rat Laryngeal Muscle," *Laryngoscope* 111, no. 3 (2001): 472–477.

17. B. Tessema, R. M. Roark, M. J. Pitman, P. Weissbrod, S. Sharma, and S. D. Schaefer, "Observations of Recurrent Laryngeal Nerve Injury and Recovery Using a Rat Model," *Laryngoscope* 119, no. 8 (2009): 1644–1651.

18. J. Hydman, S. Remahl, G. Björck, M. Svensson, and P. Mattsson, "Nimodipine Improves Reinnervation and Neuromuscular Function After Injury to the Recurrent Laryngeal Nerve in the Rat," *Annals of Otology, Rhinology & Laryngology* 116, no. 8 (2007): 623–630.

19. F. F. Chou, C. Y. Su, S. F. Jeng, K. L. Hsu, and K. Y. Lu, "Neurorrhaphy of the Recurrent Laryngeal Nerve," *Journal of the American College of Surgeons* 197, no. 1 (July 2003): 52–57, https://doi.org/10.1016/S1072-7515(03)00235-7.

20. J. W. Hong, T. S. Roh, H. S. Yoo, et al., "Outcome With Immediate Direct Anastomosis of Recurrent Laryngeal Nerves Injured During Thyroidectomy," *Laryngoscope* 124, no. 6 (June 2014): 1402–1408, https://doi.org/10.1002/lary.24450.

21. D. S. Oh, Y. W. Cheon, Y. R. Jeon, and D. H. Lew, "Activated Platelet-Rich Plasma Improves Fat Graft Survival in Nude Mice: A Pilot Study," *Dermatologic Surgery* 37, no. 5 (May 2011): 619–625, https://doi.org/10.1111/j.1524-4725.2011.01953.x.

22. C. Zheng, Q. Zhu, X. Liu, et al., "Effect of Platelet-Rich Plasma (PRP) Concentration on Proliferation, Neurotrophic Function and Migration of Schwann Cells In Vitro," *Journal of Tissue Engineering and Regenerative Medicine* 10, no. 5 (May 2016): 428–436, https://doi.org/10.1002/term.1756.

23. Y. Sowa, T. Kishida, K. Tomita, K. Yamamoto, T. Numajiri, and O. Mazda, "Direct Conversion of Human Fibroblasts into Schwann Cells that Facilitate Regeneration of Injured Peripheral Nerve In Vivo," *Stem Cells Translational Medicine* 6, no. 4 (April 2017): 1207–1216, https://doi.org/10.1002/sctm.16-0122.

24. A. L. Cattin, J. J. Burden, L. Van Emmenis, et al., "Macrophage-Induced Blood Vessels Guide Schwann Cell-Mediated Regeneration of Peripheral Nerves," *Cell* 162, no. 5 (August 2015): 1127–1139, https://doi.org/10.1016/j.cell.2015.07.021.

25. M. Takeuchi, N. Kamei, R. Shinomiya, et al., "Human Platelet-Rich Plasma Promotes Axon Growth in Brain-Spinal Cord Coculture," *Neuroreport* 23, no. 12 (August 2012): 712–716, https://doi.org/10.1097/WNR.0b013e3283567196.

26. S. L. Klein and K. L. Flanagan, "Sex Differences in Immune Responses," *Nature Reviews Immunology* 16, no. 10 (October 2016): 626–638, https://doi.org/10.1038/nri.2016.90.

27. V. R. Moulton, "Sex Hormones in Acquired Immunity and Autoimmune Disease," *Frontiers in Immunology* 9 (2018): 2279, https://doi.org/10.3389/fimmu.2018.02279.

28. E. Geerling, E. T. Stone, T. L. Steffen, M. Hassert, J. D. Brien, and A. K. Pinto, "Obesity Enhances Disease Severity in Female Mice Following West Nile Virus Infection," *Frontiers in Immunology* 12 (2021): 739025, https://doi.org/10.3389/fimmu.2021.739025.